Empirical formula for rates of hot pixel defects based on pixel size, sensor area and ISO

Glenn H. Chapman[*a], Rohit Thomas[a],
Zahava Koren[b], Israel Koren[b]

[a]School of Engineering Science, Simon Fraser University, 8888 University Drive, Burnaby, BC, Canada, V5A 1S6
[b]Dept. of Electrical & Computer Engineering, Univ. of Massachusetts, Amherst, MA, USA 01003

ABSTRACT

Experimentally, image sensors measurements show a continuous development of in-field permanent hot pixel defects increasing in numbers over time. In our tests we accumulated data on defects in cameras ranging from large area (>300 sq mm) DSLR's, medium sized (~40 sq mm) point and shoot, and small (20 sq mm) cell phone cameras. The results show that the rate of defects depends on the technology (APS or CCD), and on design parameters like imager area, pixel size (from 1.5 to 7 um), and gain (from ISO100 to 1600). Comparing different sensor sizes with similar pixel sizes has shown that defect rates scale linearly with sensor area, suggesting the metric of defects/year/sq mm, which we call *defect density*. A search was made to model this defect density as a function of the two parameters pixel size and ISO. The best empirical fit was obtained by a power law curve. For CCD imagers, the defect densities are proportional to the pixel size to the power of -2.25 times the ISO to the power of 0.69. For APS (CMOS) sensors the power law had the defect densities proportional to the pixel size to the power of -3.07 times the ISO raised to the power of 0.5. Extending our empirical formula to include ISO allows us to predict the expected defect development rate for a wide set of sensor parameters.

Keywords: defect imager defect detection, hot pixel development, APS/CCD defects rates, defect density, active pixel sensor APS, CCD, ISO, empirical defect rate equation

1. INTRODUCTION

Digital imager technology has become the preferred photographic process. Moreover, the push to add image sensing to products ranging from cell phones to cars increases their proliferation in embedded sensor design and drives down pixel sizes. Unfortunately, digital imagers like any other microelectronic device, develop defects over time. Unlike other digital devices, most in-field defects in digital imagers begin appearing soon after fabrication, are permanent, and their number increases continuously over the lifetime of the sensor. These faulty pixels degrade the quality of the image generated by the sensor. Although the impact of defects can be overcome by factory recalibration, this is often infeasible and prohibitively expensive for imagers used in most devices.

We have been investigating imager in-field defect development for several years now and have identified the characteristics and rate of faulty pixels [1-6]. Furthermore, based on the random locations of defective pixels, we have identified the in-field defect causal mechanism as most likely being cosmic ray damage. This helped us in the development of a better defect correction method [2,6]. In this paper we have added data from point and shoot cameras with small pixels and from cell phone cameras, for a larger range of sensor areas and pixel sizes. We now have collected enough data to identify differences in defect development rates that are related to several imager parameters such as the area of the imager array, the pixel cell size, the pixel type (CCD or CMOS), and sensor sensitivity or gain (ISO). The data in this paper allows the analysis of the important trends in imager defect development. In particular, we created an analytical equation that predicts defect rate trends as a function of both pixel

---

[*] glennc@cs.sfu.ca; phone 1-778-782-3814; fax 1-778-782-4951; http://www.ensc.sfu.ca/people/faculty/chapman/; School of Engineering Science, Simon Fraser University, 8888 University Drive, Burnaby, BC V5A 1S6, Canada

size and ISO. This new formula helps sensor designers in choosing imager parameters, taking into account the length of time the sensor is expected to be in service.

2. HOT PIXELS

Over the past 7 years [5,6], we manually calibrated many commercial cameras, including 24 Digital Single Lens Reflex (DSLRs), using dark field exposure (i.e., no illumination) to try and identify stuck-high and partially stuck defects. However, we have not found any of these stuck defect types, even though they are commonly discussed in camera forums. Instead, hot pixels were the dominant defect type. A hot pixel has an illumination-independent component that increases linearly with exposure time, and can, therefore, be identified by capturing a series of dark field images at increasing exposure times. Figure 1 demonstrates the dark response of a hot pixel by showing the normalized pixel illumination vs. the exposure time where illumination level 0 represents no illumination and level 1 represents saturation. The dark response of a good pixel should be close to 0 (with some variation due to noise in the sensor) at any exposure level, as shown by curve (a) in the figure. In addition, we have found [5] that hot pixels can be categorized into two types: standard hot pixels (see curve (b) in Figure 1), which have an illumination-independent component that increases linearly with exposure time; and partially stuck hot pixels (see curve (c) in the figure), which have an additional offset that can be observed at no exposure.
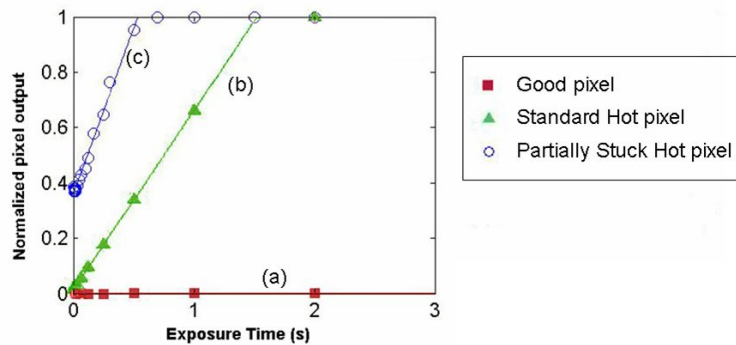
Figure 1: Comparing the dark response of a good pixel and a hot pixel.

While the overall imager system is digital, the sensor is an analog device. The response I of both a good and hot pixel can be modeled using Equation (1), where R_{photo} measures the incident illumination rate, R_{Dark} is the dark current rate, T_{exp} measures of the exposure time, b is the dark offset, and m is the amplification from the ISO setting, which is directly proportional to the ISO setting..

$$I_{Pixel}(R_{photo}, R_{Dark}, T_{exp}, b) = m \cdot (R_{photo} T_{exp} + R_{Dark} T_{exp} + b) \tag{1}$$

For ideal good pixels, both R_{Dark} and b are zero, and the output is therefore simply the measure of incident illumination. For a hot pixel, these two terms create a signal that is added on top of the incident illumination, and therefore the output from such a pixel will appear brighter. The dark response, I_{offset} of a pixel can be estimated by setting $R_{photo} = 0$, and Equation (1) then becomes

$$I_{offset}(R_{Dark}, T_{exp}, b) = m \cdot (R_{Dark} T_{exp} + b) \tag{2}$$

The expression for the dark response (also called the combined dark offset), shown in Equation (2), is linear. Therefore, by plotting the pixel dark response vs. exposure time, as shown in Figure 1, a linear function can be used to estimate R_{Dark} and b. For a standard hot pixel b is zero, and therefore, this type of defects is most visible in long exposure images. In contrast, for partially stuck hot pixels, the response depends on the magnitude of b and this type of defects will appear in all images. Obtaining this data for each camera involves typically 5 to 20 calibration images per test at a wide range of exposure times and ISO's, and their analysis with specialized software[2-4].

In our long duration study we have identified hot pixels from 24 DSLR cameras including both APS and CCD sensors, with the age of these cameras varying between 1 and 7 years [9]. After performing the dark-frame calibration at ISO 400, our results showed a cumulative total of 243 hot pixels of which 44% were of the partially stuck type. The offset in partially stuck hot pixels causes this type of defect to appear at any exposure level, and thus has a greater impact on the image quality. The imager's ISO setting controls the sensitivity or amplification of the pixel output. Higher ISO

setting enables objects to be captured under low light conditions or with very short exposures. This allows natural light photography without the need for flash or a long exposure time. The amplification level scales proportionally with the ISO setting, but the usable ISO range is limited by the noise level of the sensor. Ten years ago, most commercial DSLRs had a usable ISO range of 100 – 1600. As sensor technology improved, noise levels have been reduced and the usable ISO range has increased considerably, with recent DSLRs having a ISO range of 50 to 12,300 and high-end cameras having a range from 25,600 to 409,600 ISO.

Figure 2 shows the dark response of a hot pixel that we have measured for varying ISO levels. For low ISO. defects have low values of R_{Dark} and b. As the ISO amplification increases, both R_{Dark} and b increase dramatically, scaling linearly with the ISO (Equation 1). In fact, at ISO 12800 the dynamic range of the pixel is reduced by 40% solely due to the offset b, and at ISO 25600, the pixel is near saturation at all exposures. The high number of hot pixels with offsets suggests that the development of stuck high pixels in the field may actually be due to the presence of hot pixels with very high offsets. This is consistent with our experience of not having detected a true stuck pixel in any of our cameras, while explaining the cameras developing stuck pixels discussed in camera forums.
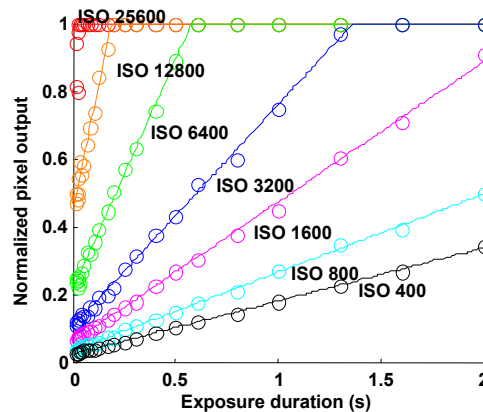
Figure 2: Dark response of a hot pixel at various ISO levels.

3. DEFECT GROWTH RATE ANALYSIS

For the growth rate analysis we need to collect data from a wide range of cameras and sensors. DSLR's cameras have large sensor areas ranging from mid frame 23x15 mm (345 mm^2) to full frame 36x24 mm (864 mm^2) with pixel sizes in the 5.5 to 7.7 microns range. This provides a large potential area for defects to develop. In our initial studies we had performed all calibrations at ISO 400, as the noise level at this setting is very small in most cameras. Based on 24 such cameras, we see in Table 1 that a total of 296 defects were found, of which 167 (56%) were offset hot pixels. The data sets that we have collected are sufficient for exploring various relationships between the defect growth rate and pixel size. As suggested by our previous analysis[9], to remove the impact of the sensor area we considered the *defect density* (D) defined as *defects per year per mm^2*, rather than the *defect rate*, which is usually defined as *defects per year (per sensor)*. The data will be summarized and analyzed using the metric D.

The ISO setting controls the sensitivity or amplification of the pixel output. Based on Equation (1), the numerical gain that is applied to the pixel output amplifies the defect parameters as well. To observe the impact of ISO on defective pixels, we have performed the dark frame calibration at different ISO levels. Due to the increase in the background noise at higher ISO, the threshold value used to identify defects was adjusted with the ISO[6]. Tables 2,3 summarize the results of our most recent calibrations on all DSLR cameras at varying ISO settings. Since our previous research has shown that CCD and APS pixels have significantly different defect rates, Table 2 summarizes these for Active Pixel Sensors while Table 3 gives the results for CCDs (note that the CCD DSLR's are mostly older styles as all new higher-end cameras are using APS). As seen in these tables, the number of identified defects increased as the ISO amplification increased. At ISO 400 we accumulated a total of 137 defects on a select group of cameras, and this almost doubled to 240 defects at ISO 800. At ISO 1600 we had a total of 367 defects, which is 2.7 times higher than the number of defects at ISO 400. This shows that at low ISO, many of the defects cannot be distinguished from noise signals but

they can be identified when the ISO is increased.   By calibrating at higher ISO, defect parameters are being amplified as in Equation (2) and the distinction between noise and defect becomes clearer.

Table 1: Summary of in-field defects from tested cameras at ISO 400.

Camera	Sensor Type	# of pixels (MP)	Sensor size (mm)	SensorArea (mm^2)	Pixel size (μm)	Age (years)	Hot Pixels		
							Standard	Partially stuck	Total
A	APS	6.3	22.7 × 15.1	342.8	7.38 × 7.36	6.4	0	26	26
B	APS	21.0	36.0 × 24.0	864.0	6.26 × 6.26	3.8	0	36	36
C	APS	6.3	22.7 × 15.1	342.8	7.38 × 7.36	4	1	5	6
D	APS	12.2	22.2 × 14.8	328.6	5.14 × 5.14	2	1	1	2
E	APS	8.0	22.2 × 14.8	328.6	6.33 × 6.33	2	0	1	1
F	APS	12.2	22.2 × 14.8	328.6	5.14 × 5.14	0.8	0	3	3
G	APS	21.0	36.0 × 24.0	864.0	6.26 × 6.96	0.5	0	1	1
H	APS	8.2	22.5 × 15.0	337.5	6.30 × 6.30	4	1	3	4
I	APS	10.1	22.2 × 14.8	328.6	5.59 × 5.59	1	0	1	1
J	CCD	6.0	23.7 × 15.5	367.4	7.96 × 7.57	4	17	0	17
K	CCD	10.0	23.6 × 15.8	372.9	5.87 × 5.87	5	6	16	22
L	CCD	10.0	23.6 × 15.8	372.9	5.87 × 5.87	5	11	23	34
M	CCD	10.0	23.6 × 15.8	372.9	5.87 × 5.87	5	12	16	28
N	CCD	10.0	23.6 × 15.8	367.4	5.87 × 5.87	2	17	1	18
O	CCD	6.0	23.7 × 15.5	372.9	7.69 × 7.57	1	0	7	7
P	CCD	6.0	23.7 × 15.5	367.4	7.69 × 7.57	2.5	9	1	10
Q	APS	8.2	22.5 × 15.0	337.5	6.30 × 6.30	2	0	2	2
R	CCD	6.0	23.7 × 15.5	367.4	7.69 × 7.57	2.5	17	0	17
S	CCD	10.0	23.6 × 15.8	372.9	6.10 × 6.10	0.5	5	6	11
T	APS	12.2	23.7 × 15.7	372.1	5.39 × 5.38	2	0	0	0
U	CCD	5.3	23.7 × 15.5	367.4	7.87 × 7.90	5	26	0	26
V	APS	18.0	22.3 × 14.9	332.3	4.30 × 4.31	2.0	1	4	5
W	APS	14.6	23.4 × 15.6	365.0	5.01 × 5.01	0.8	5	4	9
X	APS	18.0	22.3 × 14.9	332.3	4.30 × 4.31	2.0	0	10	10
Total							129	167	296

Table 2: DSLR APS Sensors defect densities (defects per year per mm^2) at various ISO levels.

Camera	Pixel (μm)	Defect Density (defects/year/mm^2)								
		100	200	400	800	1600	3200	6400	12800	25600
A	7.38	0.005470	0.007749	0.011852	0.015499	0.023704	0.020969			
B	6.26	0.004777	0.005673	0.010748	0.015226	0.017316	0.021197	0.025974	0.063592	0.114468
C	7.38		0.001459	0.003355	0.006127	0.011086				
D	5.14	0.003652	0.007305	0.011200	0.011748	0.023466				
E	6.33			0.005661	0.006513	0.015644				
F	5.14	0.003378	0.004748	0.006757	0.008766	0.014761	0.003378			
G	6.26			0.002315	0.002315	0.004630	0.004630			
H	6.30			0.002578	0.004533	0.007763				
I	6.33			0.001217	0.004870	0.009739				
Q	6.30	0.003556	0.007111	0.002281						
T	5.38									
V	4.31	0.006027	0.006027	0.007534	0.009041	0.012055	0.283291	0.412881		
W	5.01		0.007040	0.021121	0.051666	0.154969				
X	4.31	0.013789	0.013789	0.015321	0.018385	0.018385	0.140952	0.321738		

Table 3: DSLR CCD Sensors defect densities (defects per year per mm²) at various ISO levels.

Camera	Pixel (μm)	Defect Density (defects/year/mm²)								
		100	200	400	800	1600	3200	6400	12800	25600
J	7.69		0.005662	0.010508	0.014455	0.026950				
K	5.87	0.004076	0.007670	0.015260	0.021964	0.035239				
L	5.87	0.005525	0.008555	0.017968	0.025746	0.033174				
M	5.87	0.004988	0.008904	0.013356	0.023278	0.039101	0.074769			
N	7.57	0.004628	0.005689	0.026732						
O	5.87	0.005846	0.011693	0.028159						
P	7.57		0.001361	0.010372						
R	7.57			0.013883						
S	6.10			0.006785						
U	7.90			0.012141						

4. DEFECT RATES IN CAMERAS WITH SMALLER SENSORS

The number of pixels in an average commercial digital camera has increased considerably in the last 10 years. In most cameras, the size of the sensor has remained the same but the size of the pixel has been reduced significantly, thus increasing the number of pixels on the sensor. In this study we have analyzed cameras from 10 cell phones of the same type and six different types of Point and Shoot (PS) mid-priced cameras, all of which have very small sensors.

Cell phones now have very high pixel count cameras, with typical numbers for the Apple Iphone and the Samsung Galaxy S3 reaching 8 megapixels. However, to obtain this high pixel number with very low power and weight, these cell phones often have the smallest pixels, usually of APS type. The difficulty is that they also generally have very limited ability to control camera parameters such as exposure time. To test these, it was necessary for us to trick the camera exposure system by giving just the right light level for it to expose at the desired time, e.g. the maximum time for the camera. This proved very difficult to do in a repeatable manner. To solve this problem we have used a DSLR with known characteristics and an adjustable light source to get the desired setting. Thus, if we know the camera has, for example, an F2.8 lens (cell phone) and ISO 400, we can set the light to give the maximum exposure time (1/5 sec). The camera is then focused to set the exposure, the lights turned off, and the picture taken. With this new method we have been able to create a range of repeatable exposures for these cameras (both PS and cell phone). This enabled us to do a linear fit with exposure time to the hot pixel parameters and extract reliable data on the pixel behavior.

The cell phone camera we analyzed uses a 5MP APS sensor with pixel dimensions of 2.2×2.2μm, and area of 5.4x4.7 mm (23.1 mm²) which is relatively small compared to a DSLR whose pixel size is about 6.47×6.47μm and area greater than 347 mm². In addition, the cell phone cameras have very limited camera exposure and ISO control. Hence, we were only able to measure the cell phones at ISO 400. One important factor regarding our cell phones study is that we had 10 identical cameras of the same age (4 years) and characteristics, which gives more statistical significance to the data. Table 4 shows the measured defect rates over a three year period on these cell phone cameras.

As seen in Table 4, our first calibration identified a total of 117 defects in the 10 cell phone cameras. This camera is an embedded device in the cell phone, and for cost reasons, the mapping of manufacture time defects is not done as in commercial digital cameras. Thus, the defects found in our first calibration may include manufacture time defects in addition to those developed later. Despite the lack of defect mapping from the manufacturer, trends shown by our 2012 calibrations indicate that the total number of defects has almost doubled to 213 over this period. Taking the number of identified defects per cell phone camera for each calibration, we did a regression fit on the data to get the defect rate for each phone. This fit gave us both the initial number of defects (at manufacture time) and the defect rate (defects/year). The resulting average defect growth rate for the cell phone cameras was calculated to be 4.45 defects/year, and the defect density (defects/year/mm²) was 0.193, much higher than the average 0.02 for DSLR's at 400 ISO. Unfortunately, this year almost 50% of these cameras suffered a failure in their electronics so we are down

to 5 cameras to test in the future. We are starting the measurements on newer phones, with smaller pixels, but tests on these are still ongoing and are not conclusive at this point.

Table 4. Accumulated defects, defect rates, and defect densities from 10 cell phone cameras (ISO400).

Cell phone	2008	2011	Defect Rate (defects/year)	Defect Density (defects/year/mm^2)
Phone A	9	20	3.81	0.164864
Phone B	13	21	4.13	0.178711
Phone C	8	12	3.44	0.148853
Phone D	6	29	4.94	0.213760
Phone E	12	31	5.63	0.243617
Phone F	14	15	3.94	0.170489
Phone G	14	14	4.13	0.178711
Phone H	10	23	4.81	0.208135
Phone I	14	17	4.63	0.200346
Phone J	17	23	5.06	0.218953
Cumulative Total:	*117*	*205*		
Average of cell phones	*12*	*20.5*	**4.45**	**0.192557**

In addition to cell phone cameras, we have identified defects in a set of point and shoot (PS) cameras with a CCD sensor, areas ranging from 20 to 40 mm^2, pixel sizes from 1.5 to 2.8μm, and age between 1 and 7 years. To obtain data in the gap between these smaller 2 μm pixels and the much larger DSLR's (~6 μm) we obtained cameras PS-E, PS-F with pixels in the 3.3 micron range, and ages of 9 and 11 years. In the PS cameras we were able to calibrate most of the cameras at various ISO levels.

To identify defects in these cameras, the dark frame calibration procedure used for DSLRs cannot be applied because of the limited controls and functions available. In particular, the cell phone cameras do not have explicit exposure control and therefore we cannot conclude whether an identified fault is a hot pixel or a stuck high defect. More importantly, these simple cameras do not provide the raw format function, and therefore all dark images are captured in color mode. Color images generated by digital cameras are often processed with various imaging functions such as demosaicing, noise reduction, white balance, and alike. These imaging functions tend to distort the faulty pixel, causing a single pixel defect to appear as a virtual cluster. To overcome this, we designed a new calibration procedure for these cameras.

Table 5 shows the number of defects identified in the set of PS cameras. By comparing the number of defects found in the cell phone and PS cameras with the number found in the commercial DSLRs, we can gain insight into the impact on defects of reduced pixel size.

Table 5: Defect densities (defects/year/mm^2) for point-and-shoot at various ISO levels.

Camera	Sensor Type	Age (year)	Sensor size (mm)	Sensor area (mm^2)	Pixel Size (um)	Defect Density (defects/year/mm^2)		
						ISO 100	ISO 200	ISO 400
PS-A	CCD	3	7.18 × 5.32	38.2	1.97	0.049215	0.049215	0.077225
PS-B	CCD	6	5.75 × 4.31	24.8	2.81	0.063710	0.069758	0.171774
PS-C	CCD	7	5.27 × 3.96	20.9	2.57	0.040670	0.047847	0.067943
PS-D	CCD	1	6.13 4.60	28.2	1.54			0.669504
PS-E	CCD	11	5.31 × 3.98	21.2	3.32	0.041705		
PS-F	CCD	9	5.31 × 3.98	21.2	3.32	0.047252		0.105005

We have previously [4-6, 9,10] shown that the mechanism for defect creation is most likely a random process, such as cosmic rays. Other authors [7,8] have also confirmed that pixel damage that behaves as hot pixels appears to have come from the neutron component of the cosmic rays. This is in agreement with the clear indication that the defect rate scales with the sensor area, as the cosmic ray total flux per area is a random process, with very slow changes over time in a given location. Thus we must model how the changes in pixel size are affected by this almost steady flux.

5. MODELING THE TRADEOFF BETWEEN DEFECT RATE AND PIXEL SIZE

The data sets that we have collected are sufficient for exploring various relationships between the defect growth rate and pixel size. As suggested by our previous analysis[9, 10], to remove the impact of the sensor area we considered the *defect density* (D, defined as *defects per year per mm²*) versus the pixel size (S in microns) for all tested cameras for ISO 400, where we have the most data points. Note that all the cameras, including the cell phones, were treated as separate data points in this analysis. Table 2 (APS-DSLR), Table 3 (CCD-DSLR), Table 4 (cell phone) and Table 5 (Point and Shoot) give the defect densities for each camera type for a range of ISO's. Note that when scaled with area, the defect densities for small (2 μm) pixels of the cell phones and point and shoot cameras are in the order of 10 to 20 times greater than those for the DSLR's (5-7 μm pixels). Also note the growth in defect rates with increasing ISO for the same camera types

Previously, in a preliminary exploration reported in [6] and a more detailed one in [9] using the defect rates at ISO 400, we plotted D against the pixel size S. In [9], visual inspection of the *defect density D* plot showed that *D* increases rapidly as the *pixel size S* decreases, and that this increase is not linear in the pixel size. Again in [9], we showed that the best fit for the APS sensors, for the CCD sensors, and for the combined date is obtained by (the equivalent) Equations (3) and (4),

$$log(D)=log(A) + B \, log(S) \qquad (3)$$
$$D=A \, S^B \qquad (4)$$

Figure 3 shows the resulting fit to equation (4) for all the APS sensors, while Figure 4 shows the result for CCD sensors. The regression statistics from the log-log plot are summarized in Table 6. The R^2, which measures the goodness-of-fit, is 0.769. If the measure of R^2 is close to 1, it indicates that the fitted function is a close approximation to the observed values. For the combined fit of the all the pixels (both CCD and APS), $R^2 = 0.769$ indicates that the power function provides a very good fit. The residuals of the fit plot show that the deviations are nearly uniformly distributed about the fit, suggesting that the power law is a good expression fit to the data. The power B indicates that the defect density does not scale linearly with the pixel size; Instead, it increases in a power law as the pixel size decreases. The exponent factor of -2.811 suggests that the defect density scales by more than the pixel area. The t ratio (ratio of B standard error to B value) is 10.4, which shows that the power is highly significant.
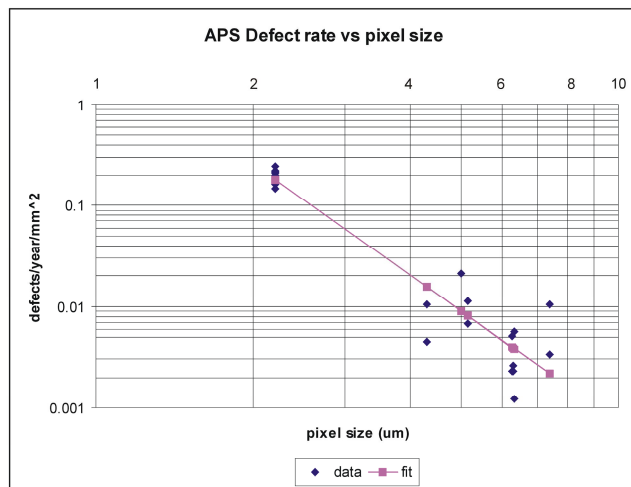
Figure 3: APS Defect density vs pixel size for ISO 400
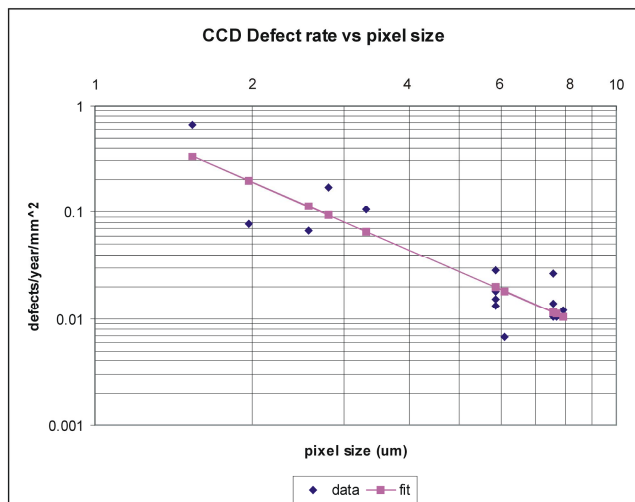
Figure 4: CCD Defect density vs pixel size for ISO 400

Table 6: Defect density vs pixel size power law fits for combined, APS and CCD sensors

Sensor Type	A (defects/mm²/year)	B (μm⁻¹)	R²
APS & CCD	1.462	-2.811	0.769
APS	3.124	-3.632	0.907
CCD	0.823	-2.109	0.812

As shown in previous results[9], the defect densities we calculated indicate that the mid-size CCDs developed 3x more defects than the mid-size APS sensors. Hence, in the following plots, we separate the results by the sensor type. The log-log plot of defect density versus pixel size of all tested APS sensors is shown in Figure 3, and for CCD sensors in Figure 4 (both for 400 ISO). Again, a linear regression fit is used and the parameters of the two fit functions are summarized in the second and third rows of Table 6.

All the data points in Figure 3 lie closely to the regression fit function. The R^2 recorded in Table 6 for the CCD is 0.81 while that for the APS is even higher at 0.91, both of which are better than the fit shown for the combined data. Since both the APS and CCD sensors show the same good regression fit with the power function, this strongly indicates that defect densities increase in a power law with the shrinkage of pixel size. The power factor B estimated for the CCDs is -2.11 which shows that the defect density scales approximately inversely with the pixel area. However, the power factor B for the APSs is -3.63, which indicates that the impact of scaling down the pixel size on an APS sensor is much greater than just the decrease in area. In both cases the t ratio is between 7.5 and 14, showing that the accuracy of these B values is high compared to the difference between them.

Another important factor to look at is the coefficient A. In this power equation, A is the number of defects/year/mm^2 when the pixel size is 1 μm. It is important to note that at 1 micron pixels, the APS is showing 3.12 defects/year/mm^2 while the CCD is showing a much lower 0.823. This is a consequence of the much stronger power growth as pixel size shrinks for the APS than for the CCD. Thus, while the CCD cameras have nearly 3 times higher defect densities at the 6 μm pixels, at 1 μm the APS defect density would be 3.8 times greater than that of CCD. Indeed these equations project that for ISO 400 at 2.4 µm pixels the number of defects/year/mm^2 would be about the same for CCD and APS pixels.

An important question is whether the same relationship holds at other ISOs? We now have sufficient data to check this for the full ISO range and both CCD and APS pixels. Previously[10] we showed that as ISO increased from 100 to 400, the pixel size exponent B changed very little but the offset (A) changed significantly. Building on this, we used a software program that explores a wide range of fitting equations (several hundred) with the variables of pixel size (microns) and ISO, and fit for the APS and CCD data separately. The resulting best empirical fit (fit with the highest R^2) was clearly an extension of the power law in Equations (3) and (4) and is given by Equation (5) in the log form, which results in the power law of Equation (6).

$$log(D) = log(A) + B\ log(S) + C\ log(ISO) \tag{5}$$
$$D = A\ S^B ISO^C \tag{6}$$

The best fit parameters are listed in Table 7 with the fitted curves shown in Figures 5 and 6. These indicate some interesting trends. Note how the fitted plains for the APS (Figure 5) rise at a much sharper angle than for the CCD (Figure 6). The power factor for the pixel size is -3.052 for APS and -2.246 for CCD, both very similar to their ISO 400 results and the t ratios are very high - 13 to 14. Secondly, this size factor is multiplied by the ISO raised to the 0.505 for APS pixels, and the slightly faster 0.687 for CCD's. Hence, the CCD's are more sensitive to ISO increases than the APS's, though this difference is not statistically significant (1.5 sd).

Table 7: Defect density vs pixel size and ISO power law fits for APS and CCD sensors

Sensor Type	A	B (S power)	C (ISO power)	R^2	D=defects/mm^2/year @1 μ, ISO400
APS	0.0742	-3.052	0.505	0.714	1.527
CCD	0.0141	-2.246	0.687	0.830	0.870

Finally it is important to note how rapidly this defect density grows as the pixel size becomes smaller. Figure 7 shows the linear plot of the APS fit, and Figure 8 for the CCD. Note how at large pixel sizes (7 μm) the density changes little with ISO. At low ISO the defect density grows modestly, but then it grows rapidly as the pixel size shrinks near 2 microns. The power law nature of the variation with pixel size is well seen on the high ISO edges of these plots.

Consider the defect density for a one micron pixel, which is obtained from (6) by setting S=1 micron and ISO=400. This shows that at this small pixel size the APS will have a greater number of 1.52 defects/year/mm^2, rather than 0.864 for the CCD's at the same parameters. For a full frame APS DSLR, this gives 1320 defects per year at the standard 400 ISO

operation, while at ISO 400 the CCD and APS densities are equal for pixels of size 2.01 microns. Moreover, by ISO 25,600 a 1μm APS pixel is expected to rise to 12.5 defects/year/mm^2, for a total on the full frame camera of 10,800 defects in a year!
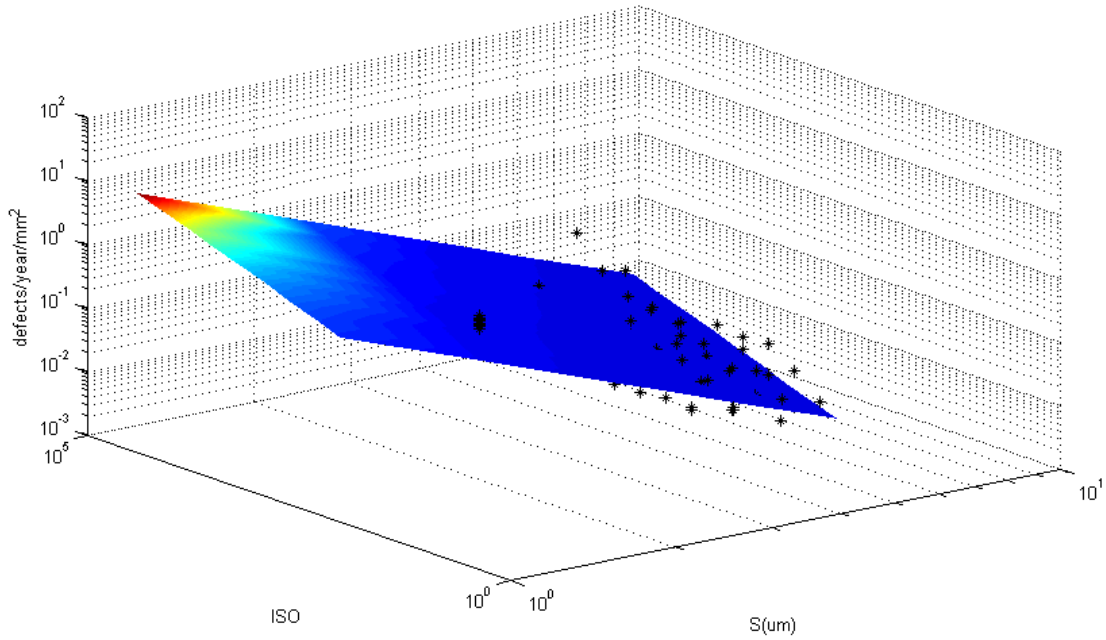
Figure 5 Fitted APS defect density vs pixel size (um) and ISO using equation (6) on log scale plots
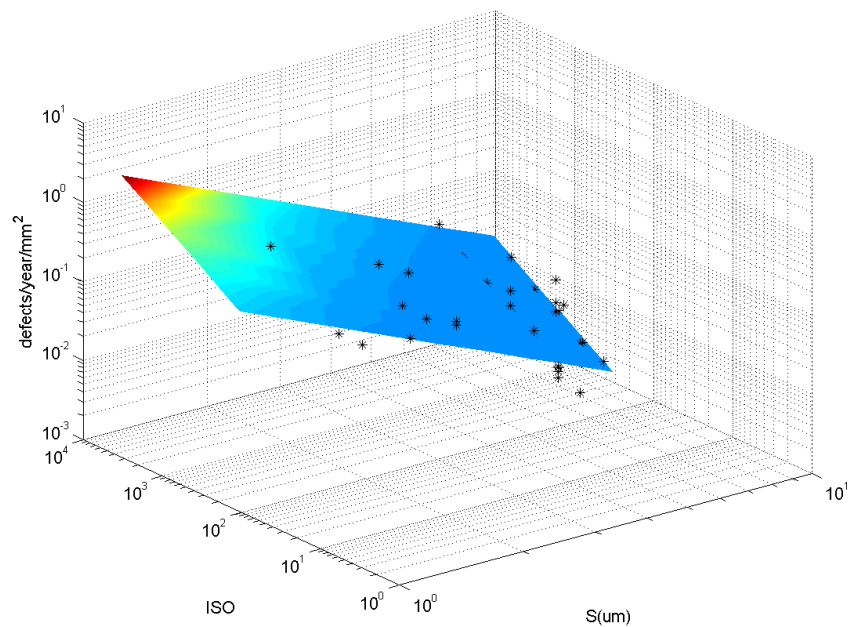
Figure 6 Fitted CCD defect density vs pixel size (um) and ISO using equation (6) on log scale plots

Indeed the warning of this fit is that below 1 micron pixels, the defect rate would require significant defect suppression for camera lifetime to be reasonable. However, at the predicted rates even the classic mapping of hot pixels and replacement by interpolation from adjacent pixels may begin to fail. Furthermore, for long operation in high radiation environments the problem will significantly worsen. Assuming that defects are actually caused by cosmic rays, defect rates could be 100 times larger for transpacific aircraft DSLR cameras, and 300 times greater in low earth orbit.
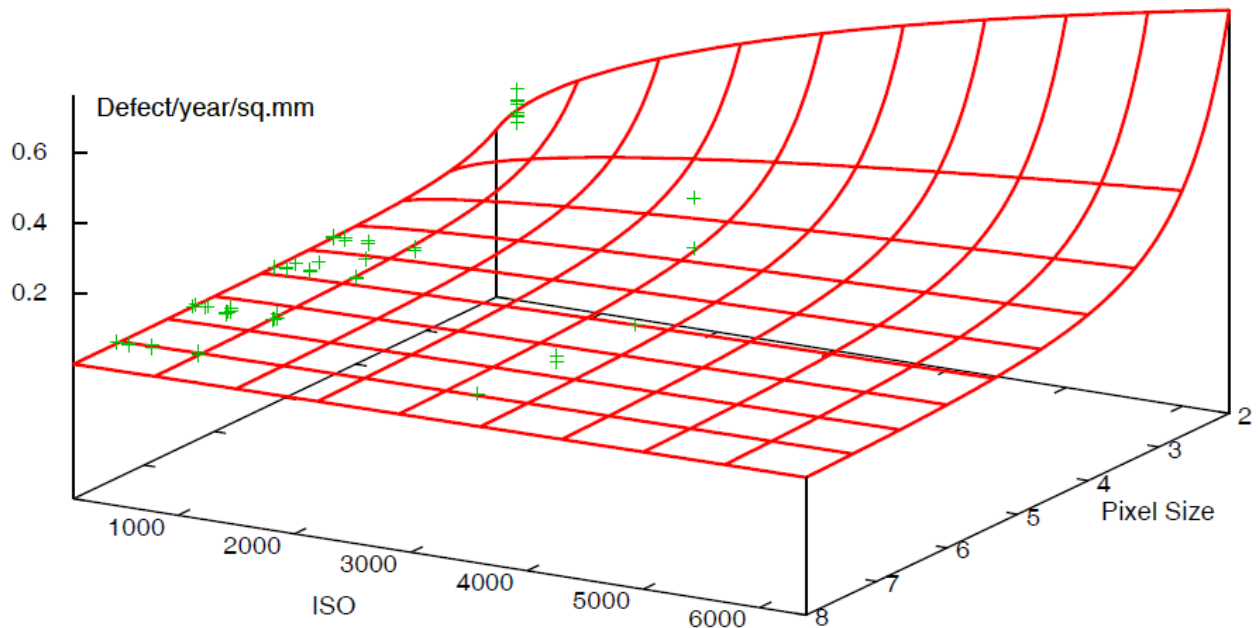
Figure 7: Fitted APS defect density vs pixel size (um) and ISO using equation (6) in a linear plot
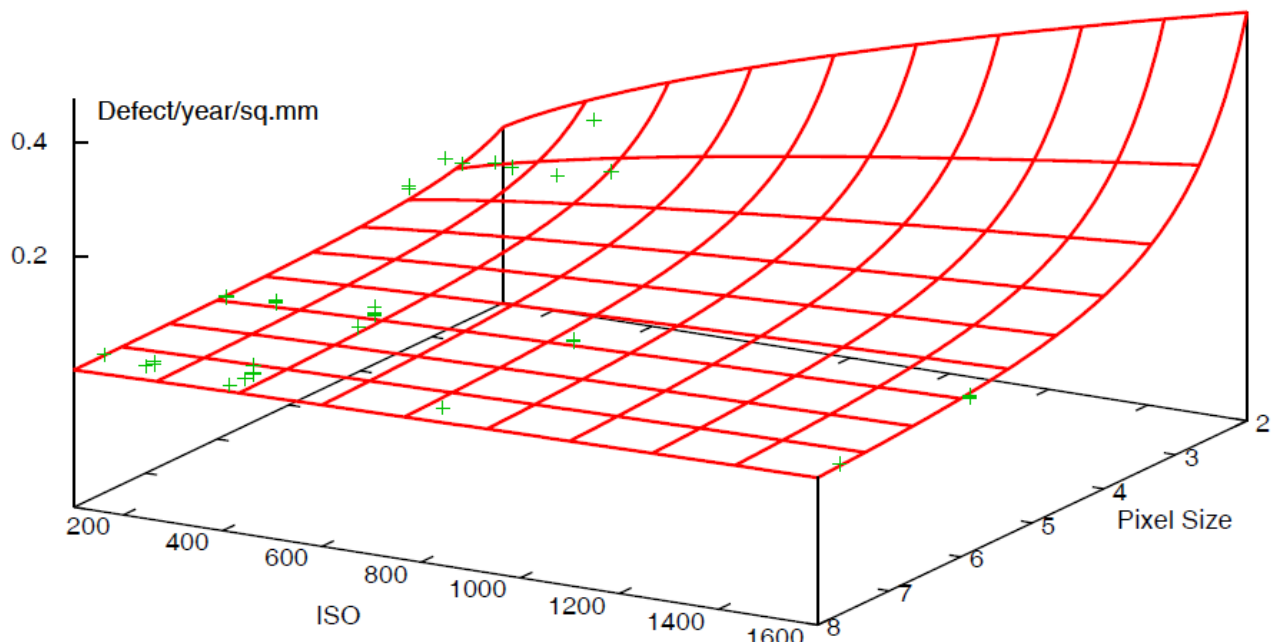
Figure 8: Fitted CCD defect density vs pixel size (um) and ISO using equation (6) in a linear plot

6. CONCLUSIONS

In our on-going study of 24 semi-professional cameras, we have observed 1416 hot pixels, of which 56% were partially stuck. In 10 cell phone cameras we found 205 hot pixels, and in 6 P&S cameras 84 hot pixels with less parameter characterization. The in-field defects were permanent and their number increased continuously over the sensor lifetime, linearly in time. To study the impact of reducing the pixel size on the rate of hot pixel generation, we analyzed a set of DSLRs with different sensor areas but similar pixel sizes (5-8 μm), cell phone cameras and mid sized point and shoot cameras with pixels in the 1.5 to 2.8 μm range.

Plotting the defect density D (defects/year/mm^2) versus both pixel size and ISO, the best fit was obtained by a power of the pixel size multiplied by a power of the ISO. The dependence of the defect density D on the pixel size is stronger than inverse to the pixel area. More importantly, we have observed that the APS defect density D grows at a much higher rate, -3.05, than the CCDs at -2.24.   Furthermore, D increases with the ISO raised to 0.505 for APS sensors and slightly faster at 0.69 for CCD's. The reason for this difference in these power relationships for CCD and APS pixels is not obvious and needs to be explored.   These formulas suggest that at about 2.01 micron pixels and ISO 400, the defect density of APS and CCD should be about equal. At 1 micron pixels, APS is projected to have much higher defect rates.

This power law relationship has important implications for designers.   We conclude that hot pixels will become a much larger issue in the near future. With more high-end DSLRs moving toward larger area sensors and higher ISO ranges, we will be observing more defects which the amplification, due to higher ISO, and the offset value of many hot pixels, will cause to appear over all exposure times.   Moreover, with the shrinkage of pixel size, defect rates would rapidly increase.   The combination of ISO expansion, sensor area increase and pixel size shrinkage will all significantly increase the rate of hot pixel defect development in cameras and sensors.

This suggests important tradeoffs in sensor design parameters that the imager designer should take into account, especially for sensors designed to last for a very long time without any calibration.   In particular it shows that shrinking the pixel size to gain number of pixels in a given sensor area, will result in defect rates growing faster than the pixel numbers, especially for APS sensors.   Thus designers must ask how many defects they can withstand over the lifetime of the sensor before the image degrades.   Moreover, if the suggested cosmic ray source of defects is correct, this has important implications for designers with applications in high radiation environments such as high altitude aircraft and earth orbit or beyond, where cosmic radiation levels are significantly higher.   These formulas give designers working in all these areas a guide for the expected defect numbers during the lifetime of their system.

REFERENCES

[1]   J. Dudas, L.M. Wu, C. Jung, G.H. Chapman, Z. Koren, and I. Koren, "Identification of in-field defect development in digital image sensors," *Proc. Electronic Imaging, Digital Photography III*, v6502, 65020Y1-0Y12, San Jose, Jan 2007.

[2]   J. Leung, G.H. Chapman, I. Koren, and Z. Koren, "Statistical Identification and Analysis of Defect Development in Digital Imagers," *Proc. SPIE Electronic Imaging, Digital Photography V*, v7250, 742903-1 – 03-12, San Jose, Jan 2009.

[3]   J. Leung, G. Chapman, I. Koren, and Z. Koren, "Automatic Detection of In-field Defect Growth in Image Sensors," *Proc. of the 2008 IEEE Intern. Symposium on Defect and Fault Tolerance in VLSI Systems*, 220-228, Boston, MA, Oct. 2008.

[4]   J. Leung, G. H. Chapman, I. Koren, Z. Koren, "Tradeoffs in imager design with respect to pixel defect rates," *Proc. of the 2010 Intern. Symposium on Defect and Fault Tolerance in VLSI*, 231-239., Kyoto, Japan, Oct 2010.

[5]   J. Leung, J. Dudas, G. H. Chapman, I. Koren, Z. Koren, "Quantitative Analysis of In-Field Defects in Image Sensor Arrays," *Proc. of the 2007 Intern. Symposium on Defect and Fault Tolerance in VLSI*, 526-534, Rome, Italy, Sept 2007.

[6]   J. Leung, G.H. Chapman, Y.H. Choi, R. Thomson, I. Koren, and Z. Koren, "Analyzing the impact of ISO on digital imager defects with an automatic defect trace algorithm", *Proc. Electronic Imaging, Sensors, Cameras, and Systems for Industrial/Scientific Applications XI*, v 7536, 75360F1-0F12, San Jose, Jan. 2010

[7]   A.J.P. Theuwissen, "Influence of terrestrial cosmic rays on the reliability of CCD image sensors. Part 1: experiments at room temperature," *IEEE Transactions on Electron Devices*, Vol. 54 (12), 3260-6, 2007.

[8]   A.J.P. Theuwissen, "Influence of terrestrial cosmic rays on the reliability of CCD image sensors. Part 2: experiments at elevated temperature," *IEEE Transactions on Electron Devices*, Vol. 55 (9), 2324-8, 2008.

[9]   G.H. Chapman, J. Leung, A. Namburete, I. Koren and Z. Koren," Predicting pixel defect rates based on image sensor parameters", *Proc. IEEE Int. Symposium on Defect and Fault Tolerance*, 408-416, Vancouver, Canada, Oct. 2011.

[10]   G.H. Chapman, J. Leung, R. Thomas, I. Koren, and Z. Koren, "Projecting pixel defect rates based on pixel size, sensor area and ISO", *Proc. Electronic Imaging, Sensors, Cameras, and Systems for Industrial/Scientific Applications XII*, v8298, 82980E-1-E-11, San Francisco, Jan 2012